JMEPEG (2008) 17:163–167
DOI: 10.1007/s11665-007-9180-6

1059-9495/$19.00

# Impact of Selective Grain Refinement on Superplastic Deformation: Finite Element Analysis

*Mohammad A. Nazzal and Marwan K. Khraisheh*

*(Submitted September 19, 2007)*

**Recently, Friction Stir Processing has been introduced as an effective tool to refine the grain structure of sheet metals and enhance their superplasticity. A possible application of friction stir processing is selective grain refinement to enhance deformation uniformity and minimize localized thinning. This selective treatment will result in a sheet with grain size gradient. Very limited studies have been directed toward investigating the effect of grain size gradient on the superplastic deformation during SPF. In this work, Finite Element simulations for the free bulging of a dome made of 7075Al alloy were conducted to examine the effects of initial grain size gradient within the sheet on SPF characteristics. The results clearly demonstrate that selective grain refinement can be utilized to eliminate severe thinning and improve the integrity of the superplastic formed part.**

**Keywords** finite element analysis, selective grain refinement, superplastic forming

## 1. Introduction

Superplastic forming (SPF) is a continually developing manufacturing technique that has been utilized most effectively in the aerospace industry (Ref 1). The most common form of SPF is blow forming of heated sheets into a single surface die using pressurized gas. Despite the several advantages of SPF that include greater design flexibility, low forming pressure, low die costs, and minimization of fasteners and fixtures, its industrial use is still limited. This is due to a number of reasons such as low production rates due to the low strain rates experienced during SPF, non-uniform sheet thickness distribution, and severe thinning that occurs in some regions of the formed part.

Grain size refinement of sheet metals enhances superplasticity, increases the strain rate sensitivity index, and shifts the optimum strain rate to a higher value (Fig. 1) which facilitates mass production of superplastic formed parts. Friction Stir Processing (FSP) is an emerging material processing technique used to refine and homogenize the microstructure of sheet metals. FSP is a solid-state process in which a specially designed rotating cylindrical tool, consisting of a pin and a shoulder, is plunged into a sheet. The tool is then traversed in the desired direction. The rubbing of the rotating shoulder generates heat which softens the material while the mechanical stirring caused by the pin forces the material within the processed zone to undergo severe plastic deformation yielding a dynamically recrystallized fine grain microstructure (Ref 2).

Mahoney et al. (Ref 3) conducted biaxial testing of friction stir processed aluminum sheets. They carried out cone tests using pressurized gas for a friction stir processed superplastic 7475Al alloy. Their results clearly demonstrate that FSP improves the superplastic behavior of that alloy. In addition, they were able to form a full-size component made of a friction stir processed aluminum sheet using the gas blow forming technique.

It has been demonstrated experimentally that during FSP of a metal sheet, varying the process parameters, i.e., rotational and translational speeds, leads to different grain microstructures (Ref 4). Ma et al. (Ref 4) subjected the commercial 7075Al alloy to FSP with different process parameters (4 ipm/400 rpm and 6 ipm/350 rpm). They found that the resulting microstructure varies when FSP parameters are changed. The average grain size was 7.5 and 3.8 μm for processing parameters of 4 ipm/400 rpm and 6 ipm/350 rpm, respectively. Both processed alloys exhibit superplastic behavior. They also conducted high-temperature tensile tests for the FSP alloys. The stress-strain rate curves for the processed alloys show that for the same strain rate, the flow stress is lower for the alloy with an average grain size of 3.8 μm when compared to the one with an average grain size of 7.5 μm. The flow stress of the material affects the forming pressure during SPF; for the same set of geometrical parameters, higher pressure is needed to form the sheet that has higher flow stress. This means if a certain amount of forming pressure is applied to the two processed sheets, the strain rate obtained in the 3.8 μm-sheet will be much higher than that obtained in the 7.5 μm-7075Al sheet. In other words, the material will flow faster for the sheet with finer grain size. These results motivate the idea of using FSP to refine certain areas of the metal sheet so that different grain sizes are obtained within the sheet such that coarser grain structure exists in regions where severe thinning is expected to take place during SPF leading to reduced material flow.

This article was presented at the AeroMat Conference, International Symposium on Superplasticity and Superplastic Forming (SPF) held in Baltimore, MD, June 25-28, 2007.

**Mohammad A. Nazzal** and **Marwan K. Khraisheh**, Center for Manufacturing & Department of Mechanical Engineering, University of Kentucky, Lexington, KY 40506-0108. Contact e-mail: khraisheh@engr.uky.edu.

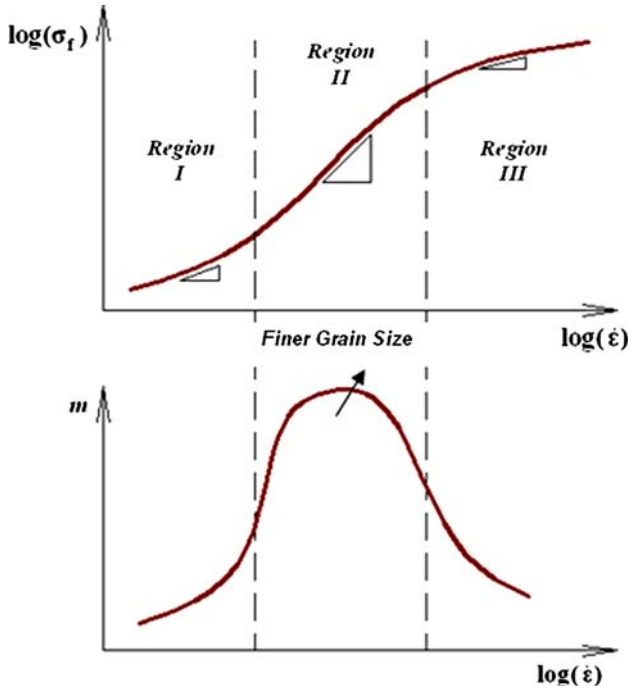


**Fig. 1** Typical stress-strain rate curve for superplastic materials

The main objective of this work is to study the effects of varying the initial grain size within the sheet on the SPF characteristics using Finite Element (FE) analysis. The analysis is conducted for the 7075Al alloy at 480 °C and the experimental data are taken from Ma et al. (Ref 4). A brief overview of the constitutive model is first given followed by a detailed FE analysis for different forming scenarios.

## 2. FE Model

The FE simulations are performed using the commercial finite element solver ABAQUS version 6.5. This FE code includes direct implicit integration, which is chosen for superplastic analysis since it enables a full static solution of deformation problems with convergence control. In addition, the time increment size can be defined with practical limits. A built-in pressure control algorithm aimed at obtaining a practical load curve at low computational cost is used in the analysis. Details on this algorithm can be found elsewhere (Ref 5).

Two user-defined subroutines (Ref 5) were developed to define the material viscoplastic behavior that has the following form which accounts for grain growth during deformation (Ref 5, 6):

$$\dot{\bar{\varepsilon}} = \frac{k}{d^p}\bar{\sigma}^{1/m} \quad \text{(Eq 1)}$$

$$d = d_0 + c\bar{\varepsilon} \quad \text{(Eq 2)}$$

where $\bar{\varepsilon}$ and $\dot{\bar{\varepsilon}}$ are the effective strain and strain rate, respectively, $\bar{\sigma}$ is the effective flow stress, $m$ is the strain rate sensitivity index, $p$ is the grain growth exponent, $d$ is the average grain size, $d_0$ is the initial grain size, and $k$ and $c$ are material parameters. A simple linear evolution equation for grain size ($d$) is used and cavitation is not accounted for in this model.

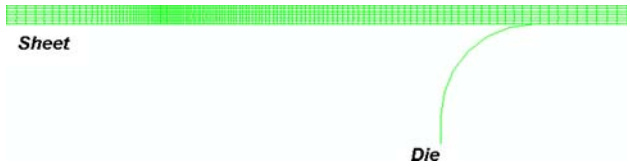


**Fig. 2** FE model

**Table 1 List of material parameters for 3.8 μm-7075Al alloy used in the simulations. These parameters were fitted to the experimental data of Ma et al. (Ref 4)**

| Material parameter | Value |
|---|---|
| $m$ | 0.57 |
| $d_0$ | 3.8 |
| $p$ | 2 |
| $k$ | $3.979 \times 10^{-14}$ |
| $c$ | 4.33 |

**Table 2 List of material parameters for 7.5 μm-7075Al alloy used in the simulations. These parameters were fitted to the experimental data of Ma et al. (Ref 4)**

| Material parameter | Value |
|---|---|
| $m$ | 0.4 |
| $d_0$ | 7.5 |
| $p$ | 2 |
| $k$ | $1.757 \times 10^{-16}$ |
| $c$ | 4.33 |

FE simulations for the free bulging of a dome are conducted in this study. The free forming region of the die is 17 cm in diameter, and the initial sheet thickness is 3 mm. Taking advantage of symmetry, an axisymmetric FE model is used as shown in Fig. 2. The die is modeled as a rigid body. A total of 804 axisymmetric four-node bilinear continuum elements are used to model the sheet. A very fine mesh is used in the transition region between the fine and coarse grains to enhance the analysis accuracy. The reason for using continuum elements is to capture the multiaxial stress state generated in the transition region. The load is controlled according to the maximum strain rate found in the sheet, which is set to $2.5 \times 10^{-3}$ $s^{-1}$. For all simulations, the analysis is stopped when the dome height reaches 7.5 cm.

## 3. Discussion and Results

FE simulations of superplastic forming of friction stir processed 7075Al sheet at 480 °C are conducted. The material parameters used in simulations are obtained by fitting the model to the experimental data obtained from Ma et al. (Ref 4). Tables 1 and 2 list the material parameters. As mentioned before, Ma et al. (Ref 4) obtained different grain microstructures by varying the FSP parameters. An average grain size of 7.5 and 3.8 μm was achieved for processing parameters of 4 ipm/400 rpm and 6 ipm/350 rpm, respectively. The stress-strain rate curves for the 7.5 μm-7075Al and 3.8 μm-7075Al

alloys are shown in Fig. 3 (Ref 4). It is observed from this figure that the strain rate sensitivity index, which is the slope of the stress-strain curve, is higher for the 3.8 μm-7075Al alloy when compared to the 7.5 μm-7075Al alloy. On the other hand, the flow stress at the same strain rate is lower for the 3.8 μm-7075Al alloy.

To study the effects of varying the initial grain size within the sheet on the SPF characteristics, several simulation runs for different cases are conducted. The first four cases are as follows:

*Case 1*: In this case, SPF of the 7.5 μm-7075Al sheet is simulated.

*Case 2*: In this case, SPF of the 3.8 μm-7075Al sheet is simulated.

*Case 3*: In this case, the sheet is divided into two zones as shown in Fig. 4: Zone 1 where the initial average grain size is set to 3.8 μm (the material properties of the 3.8 μm-7075Al alloy are used), and Zone 2 where the initial average grain size is set to 7.5 μm (the material properties of the 7.5 μm-7075Al alloy are used). The radius of Zone 2 is 2.5 cm.

*Case 4*: In this case, the sheet is divided into two zones as shown in Fig. 4: Zone 1 where the initial average grain size is set to 7.5 μm and Zone 2 where the initial average grain size is set to 3.8 μm.

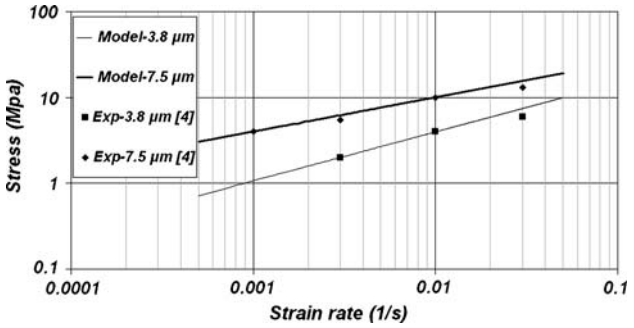


**Fig. 3** Stress-strain rate curves for the FSP 7075Al alloy: Model vs. Experimental data (Ref 4)


**Fig. 4** Die-Sheet geometry with Zones 1 and 2 highlighted

Figure 5 shows the strain rate distribution in the formed sheet for the four runs when the dome height is equal to 3.72 cm. For Cases 1 and 2, the maximum strain rate occurs at the pole of the dome, which is expected for the bulge forming of a dome because the maximum amount of deformation occurs there. For Case 3, it is observed that the strain rate in Zone 1 reaches a value of $2.5 \times 10^{-3}$ $s^{-1}$; on the other hand, the strain rate in Zone 2 which contains the pole of the dome does not exceed $5 \times 10^{-4}$ $s^{-1}$. For Case 4, it can be seen that the maximum strain rate occurs at the pole of the dome; however, the strain rate in Zone 1 is extremely low. It is depicted from this figure that the rate of change of strain with time or the rate of material flow at the polar region of the dome can be decreased by coarsening the grain size in that region when compared to the rest of the sheet. Refining the grain size in the polar region, as in Case 4, yields to more material flow of that region when compared to the rest of the sheet, which has an adverse effect on the thickness in the polar region. This makes Case 4 impractical in eliminating thinning at the polar region of the sheet.

Figure 6 shows the final through-thickness true strain, which is directly related to the sheet thickness, in the formed sheets for Cases 1 through 4. When the results obtained from Cases 1 to 2 are compared, it is seen that greater through-thickness strain in the polar region is observed for the sheet with coarser grain size. Maximum through-thickness strains of –0.867 and –0.707 are obtained for the 7.5 μm-7075Al and 3.8 μm-7075Al sheets, respectively. This is because the strain rate sensitivity is higher for the 3.8 μm-7075Al alloy when compared to the 7.5 μm-7075Al alloy. The common factor between both cases is that the thickness distribution varies smoothly; in other words, there is no sudden change in the thickness in any adjacent points in the sheet. Different results are obtained for Case 3; it is observed that the through-thickness strain in the

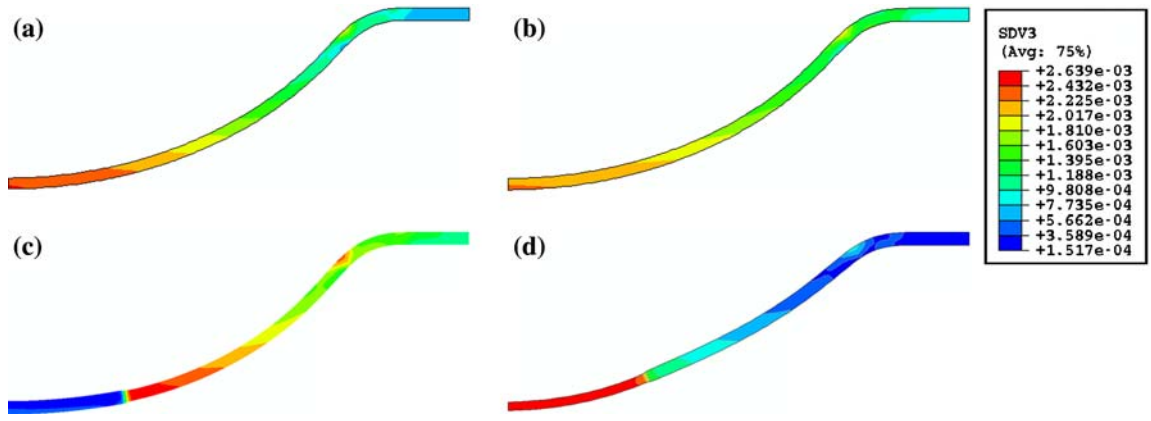


**Fig. 5** Strain rate distribution in the formed part for Cases 1 to 4. (a) Case 1: 7.5 μm-7075Al alloy. (b) Case 2: 3.8 μm-7075Al alloy. (c) Case 3: The initial average grain size in Zone 1 is 3.8 μm, the initial grain size in Zone 2 is 7.5 μm. (d) Case 4: The initial average grain size in Zone 1 is 7.5 μm, the grain size in Zone 2 is 3.8 μm

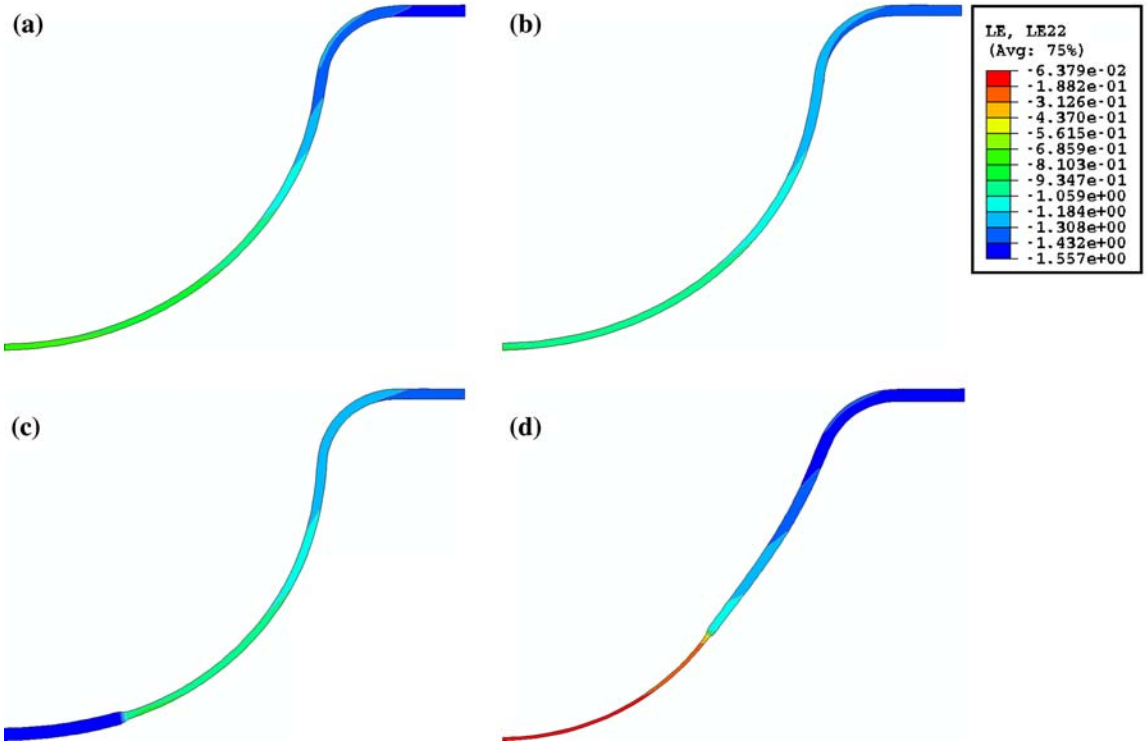


**Fig. 6** Through-thickness distribution in the formed part for Cases 1 to 4. (a) Case 1: 7.5 μm-7075Al alloy. (b) Case 2: 3.8 μm-7075Al alloy. (c) Case 3: The initial average grain size in Zone 1 is 3.8 μm, the initial grain size in Zone 2 is 7.5 μm. (d) Case 4: The initial average grain size in Zone 1 is 7.5 μm, the grain size in Zone 2 is 3.8 μm

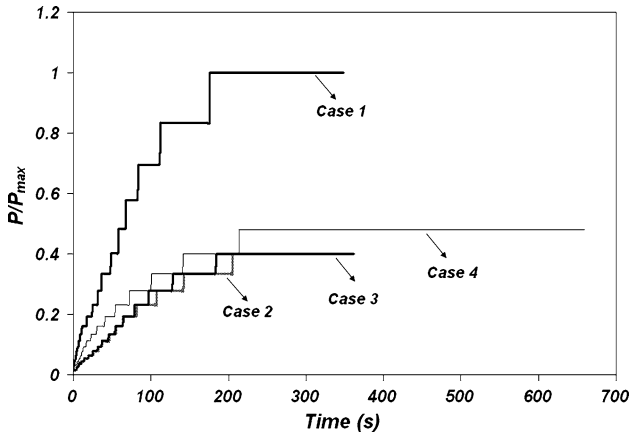


**Fig. 7** Pressure time schedules for the first four cases

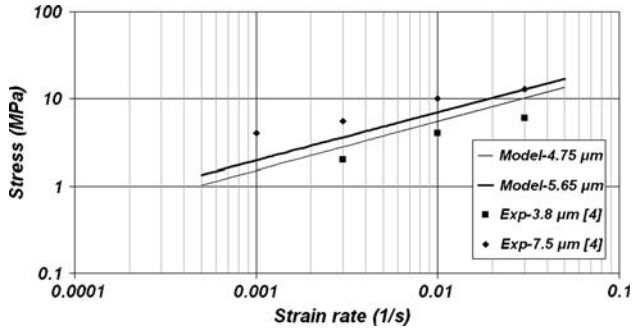


**Fig. 8** Stress-strain rate curves for the FSP 7075Al alloy with the interpolated stress-strain rate curves 5.6 μm and 4.8 μm-7075Al alloys

polar region is very small (less than −0.1). This is because the strain rate at the polar region of the dome for this specific case is lower than that in the rest of the sheet. On the other hand, high through-thickness strain (−0.7) is observed in the transition region between the fine and coarse grains. More uniformity can be achieved if the average grain size in Zone 2 is less than 7.5 μm as will be shown later. The results obtained from Case 4 show that very high through-thickness strain (−1.557) and severe thinning took place in the polar region. This is because the material flow is localized in Zone 2 which is relatively small when compared to the size of the sheet.

Figure 7 shows the pressure profiles for the four previous cases. It is seen that the pressure needed to form the part made of the 7.5 μm-7075Al alloy (Case 2) is higher than that needed for the other cases. This is because of the higher flow stress obtained when the grain size is increased. On the other hand, the forming pressure profiles for Cases 2 and 3 are comparable. It is also noticed that more time is required to form the part for Case 4 when compared to the other cases. This is expected since Case 4 is approximately equivalent to forming a 5 cm diameter sheet with an initial grain size of 3.8 μm into a 7.5 cm height dome.

In an effort to eliminate thinning at the polar region of the dome while maintaining a smooth thickness variation in the formed part, FE simulations for two cases are conducted. The two cases are as follows:

*Case 5*: In this case, the sheet is divided into two zones as shown in Figure 4: Zone (1) where the initial average

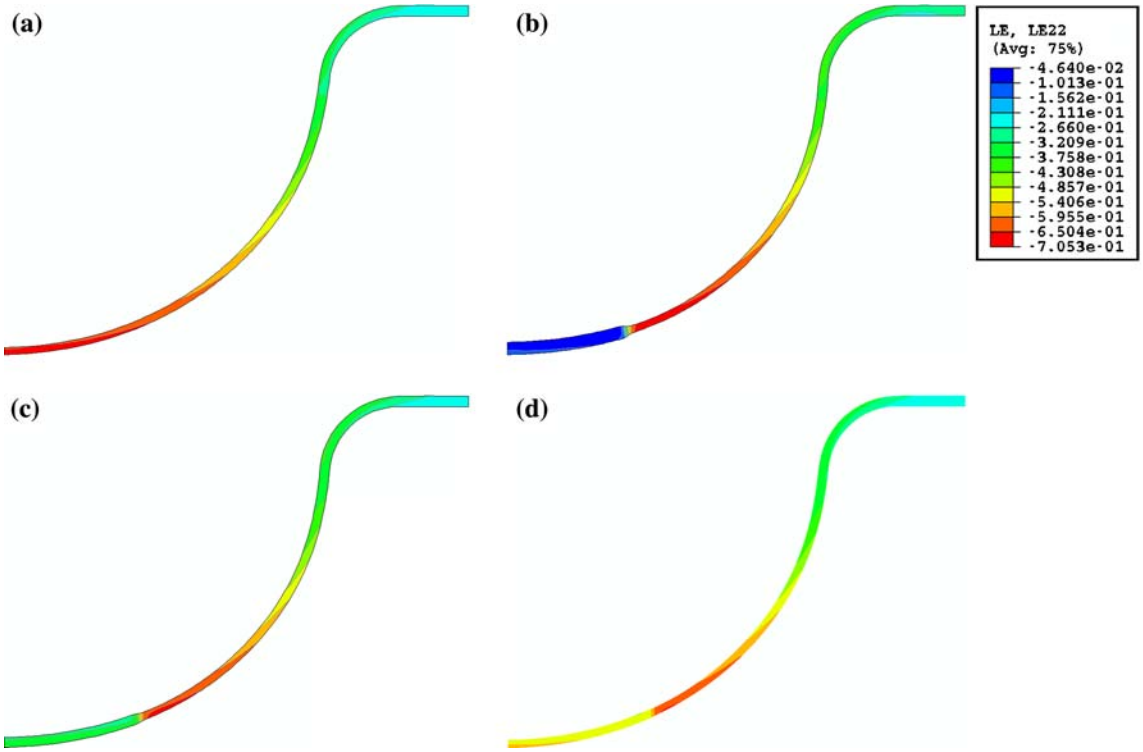


**Fig. 9** Through-thickness distribution in the formed part for Cases 2, 3, 5, and 6. (a) Case 2: 3.8 μm-7075Al alloy. (b) Case 3: The initial average grain size in Zone 1 is 3.8 μm, the initial grain size in Zone 2 is 7.5 μm. (c) Case 5: The initial average grain size in Zone 1 is 3.8 μm, the initial grain size in Zone 2 is 5.6 μm. (d) Case 6: The initial average grain size in Zone 1 is 3.8 μm, the initial grain size in Zone 2 is 4.8 μm

grain size is set to 3.8 μm, and Zone (2) where the initial average grain size is set to 5.6 μm.

*Case 6*: In this case, the sheet is divided into two zones as shown in Figure 4: Zone (1) where the initial average grain size is set to 3.8 μm, and Zone (2) where the initial average grain size is set to 4.8 μm.

Linear interpolation is used to obtain the material properties and stress-strain rate curves for the 5.6 μm and 4.8 μm-7075Al alloys. The stress-strain rate curves for those alloys are shown in Fig. 8. Figure 9 shows the through-thickness strain distribution in the formed sheet for Cases 2, 3, 5, 6. It is seen from this figure that if the initial grain size in Zone 2 is increased, less thinning in the polar region will be achieved. However, if the initial grain size in Zone 2 is increased above certain limits, severe thinning and premature failure will take place in Zone 1, specifically in the region adjacent to Zone 2. On the other hand, it can be seen that as the initial grain size in Zone 2 approaches the initial grain size in Zone 1 as in Case 6, the improvement in the thickness distribution at the polar region becomes less significant. Thus, the initial grain size distribution in the sheet has to be carefully determined in order to achieve the desired specifications.

## 4. Conclusions

The effects of varying the initial grain size within the formed sheet on the SPF characteristics using FE analysis are studied. The FE simulations show that FSP can be used as a powerful tool to eliminate localized thinning in the superplastic formed part. However, the grain size gradient has to be carefully determined so that localized thinning is not shifted from one region to another. Therefore, the FE simulation of SPF can provide valuable information about the initial grain size requirements that lead to the most uniform part.


## Acknowledgment

The support of the National Science Foundation, CAREER Award # DMI-0238712, is acknowledged.


## References


1. D.G. Sanders, The History and Current State-of-the-Art in Air frame Manufacturing Using Superplastic Forming Technologies, *Advances in Superplasticity and Superplastic Forming*, E. Taleff, P. Friedman, P. Krajewski, R. Mishra, and J. Schroth, Ed., Metals and Materials Society, 2004, p 3–8
2. B. Darras, M. Omar, and M.K. Khraisheh, Experimental Thermal Analysis of Friction Stir Processing, *Mater. Sci. Forum*, 2007, **539–543**, p 3801–3806
3. M. Mahoney, A.J. Barnes, W.H. Bingel, and C. Fuller, Superplastic Forming of 7475 Al Sheet after Friction Stir Processing, *Mater. Sci. Forum*, 2004, **447–448**, p 505–512
4. Z.Y. Ma, R.S. Mishra, and M.W. Mahoney, Superplastic Deformation Behavior of Friction Stir Processed 7075 Al Alloy, *Acta Mater.*, 2002, **50**, p 4419–4430
5. M.A. Nazzal, M.K. Khraisheh, and B.M. Darras, Finite Element Modeling and Optimization of Superplastic Forming Using Variable Strain Rate Approach, *J. Mater. Eng. Perform.*, 2004, **13**(6), p 691–699
6. C.H. Caceres and D.S. Wilkinson, Large Strain Behavior of a Superplastic Copper Alloy Deformation, *Acta Metall.*, 1984, **32**, p 415–422